

## Supporting Information

### **A simple and general approach for *in situ* synthesis of sulfur-porous carbon composites for Lithium-Sulfur batteries**

**Noel Díez, Guillermo A. Ferrero, Marta Sevilla, Antonio B. Fuentetaja\***

*Instituto Nacional del Carbón (CSIC), Fco. Pintado Fe 26, Oviedo 33011, Spain*

\*Corresponding author: [abefu@incar.csic.es](mailto:abefu@incar.csic.es)

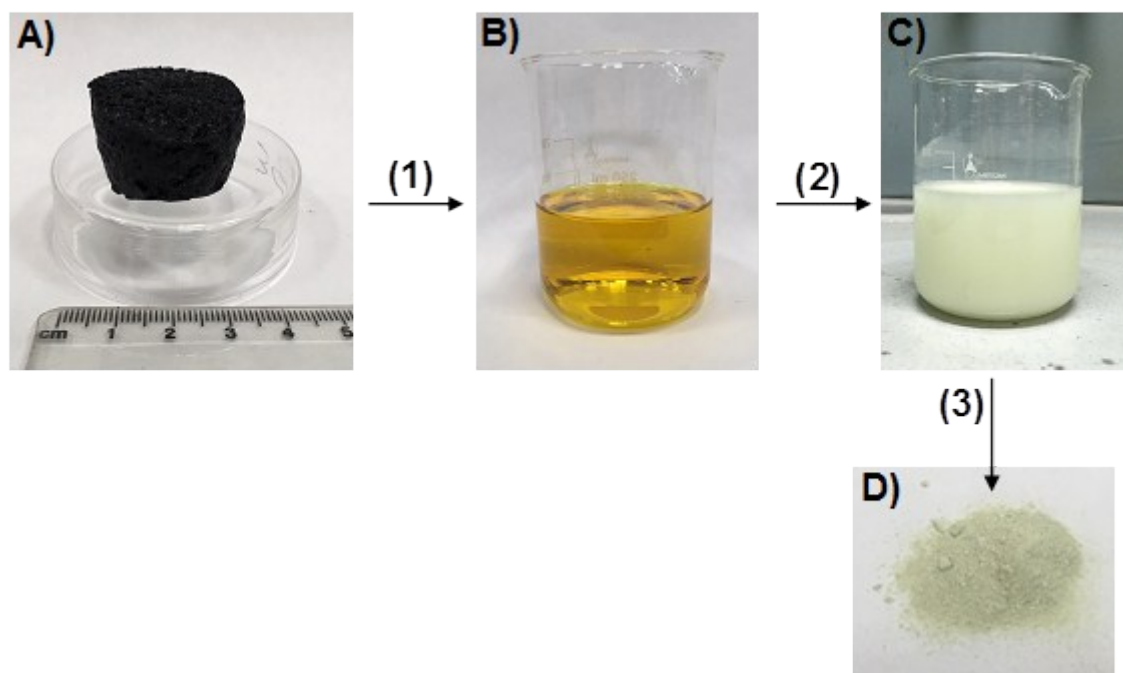


**Figure S1.** Evidence of the generation of sulfur from the carbonized solid. A) carbonized monolith, B) yellowish aqueous filtrate with sodium polysulfides, C) pale yellowish colloidal suspension of sulfur particles and D) precipitated sulfur. The steps are: (1) water washing, (2) addition of hydrochloric acid, (3) separation of sulfur by centrifugation and drying.

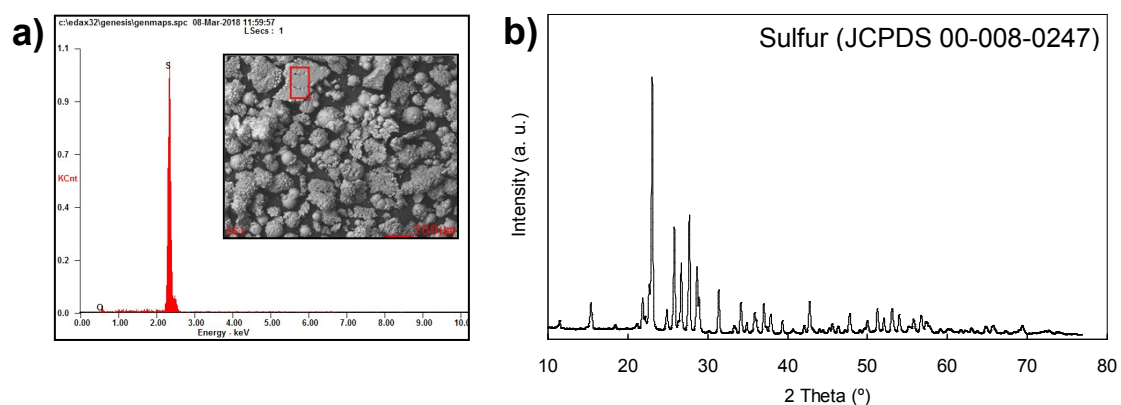


**Figure S2.** a) EDX spectrum and b) XRD pattern of recovered sulfur (Figure S1D). This pattern reveals that sulfur has an orthorhombic structure (JCPDS 00-008-0247).

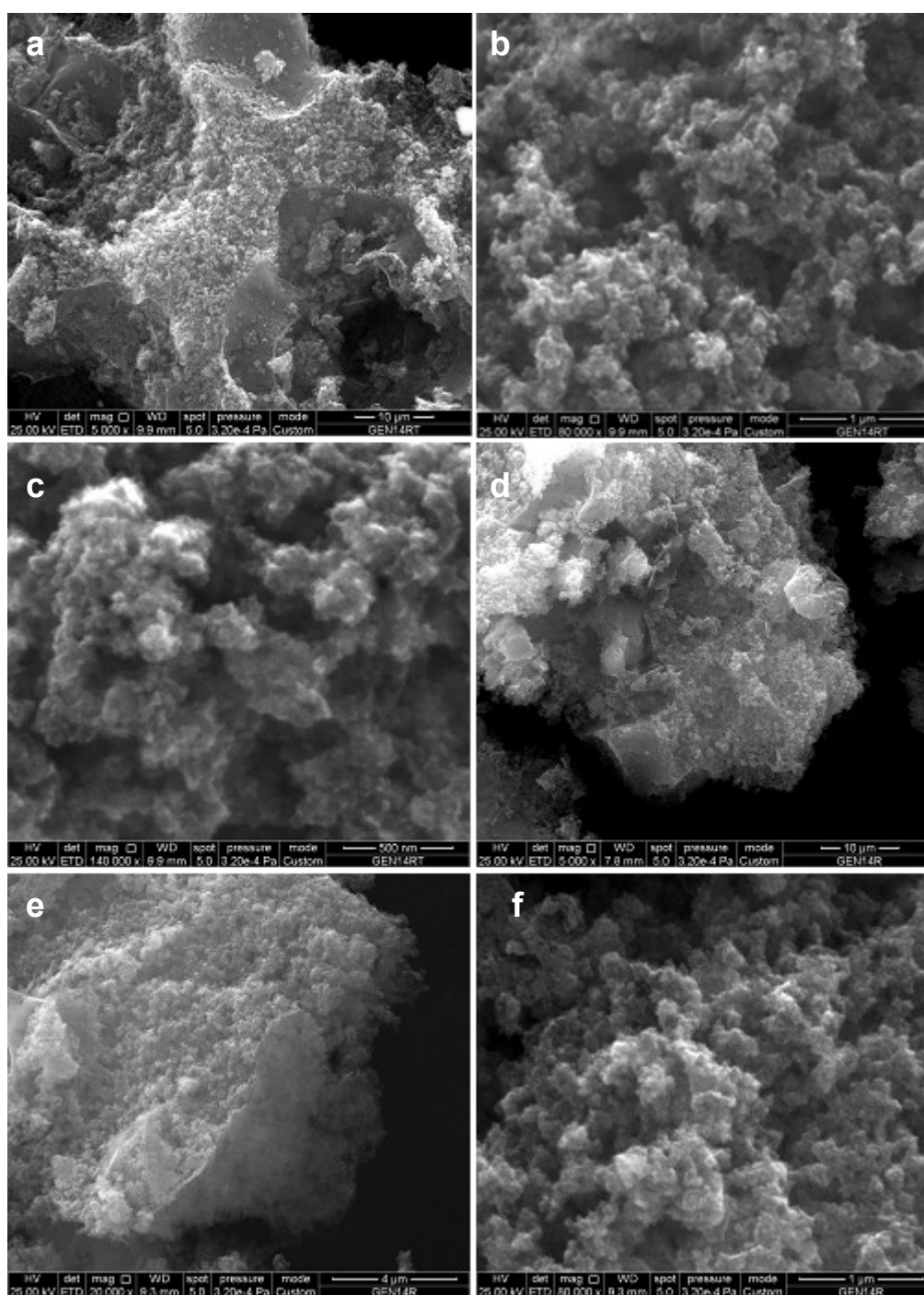


**Figure S3.** SEM images of the porous carbon C-2 (a, b and c) and the sulfur/carbon composite S/C-2 (d, e and f).

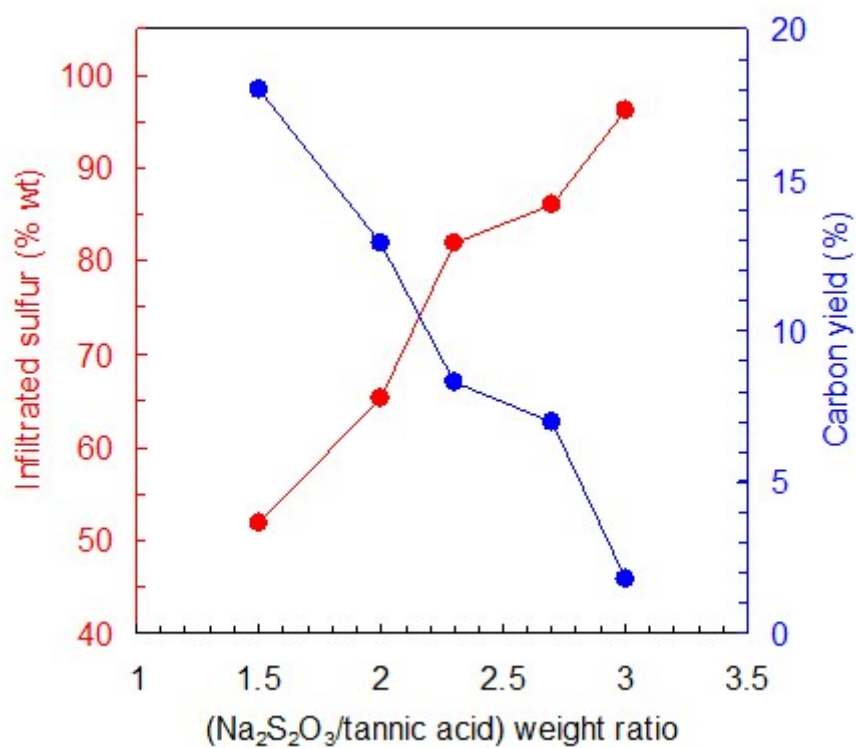


**Figure S4.** Influence of the (Na<sub>2</sub>S<sub>2</sub>O<sub>3</sub>/tannic acid) weight ratio upon the amount of sulfur infiltrated and the carbon yield.

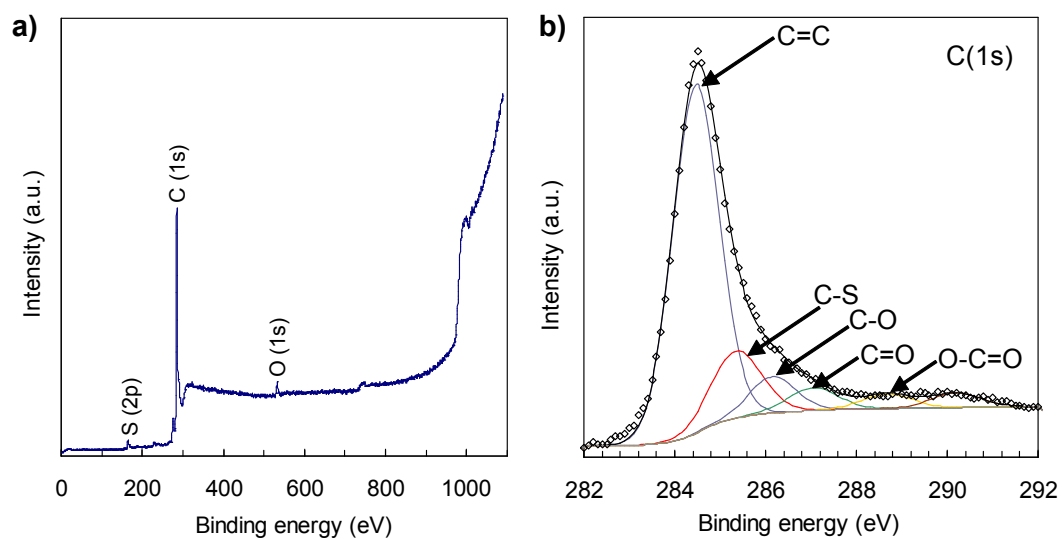


**Figure S5.** XPS analysis of the porous carbon sample C-1.5: (a) XPS survey spectrum and (b) high-resolution C 1s XPS spectrum.

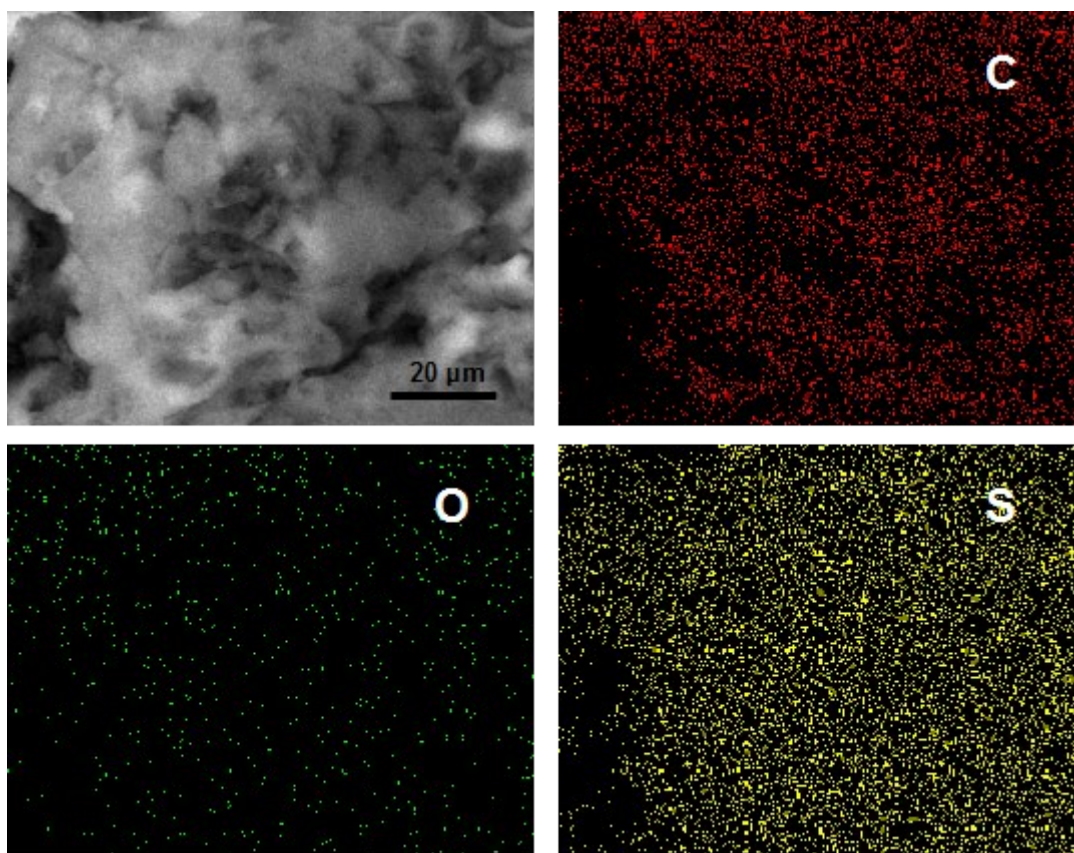


**Figure S6.** SEM-EDX mapping of C, O and S for the S-doped porous carbon sample C-1.5.

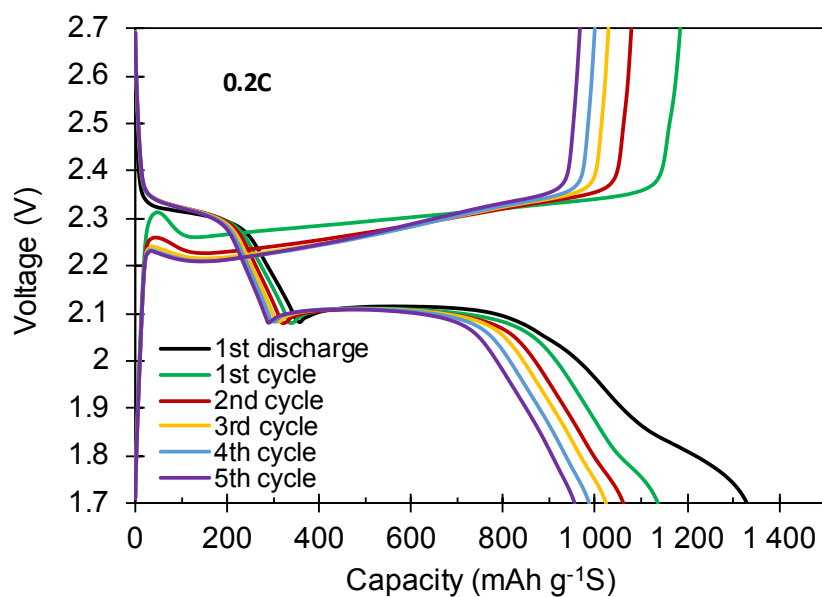


**Figure S7.** Galvanostatic charge-discharge curves recorded at 0.2 C (sample: S/C-1.5).

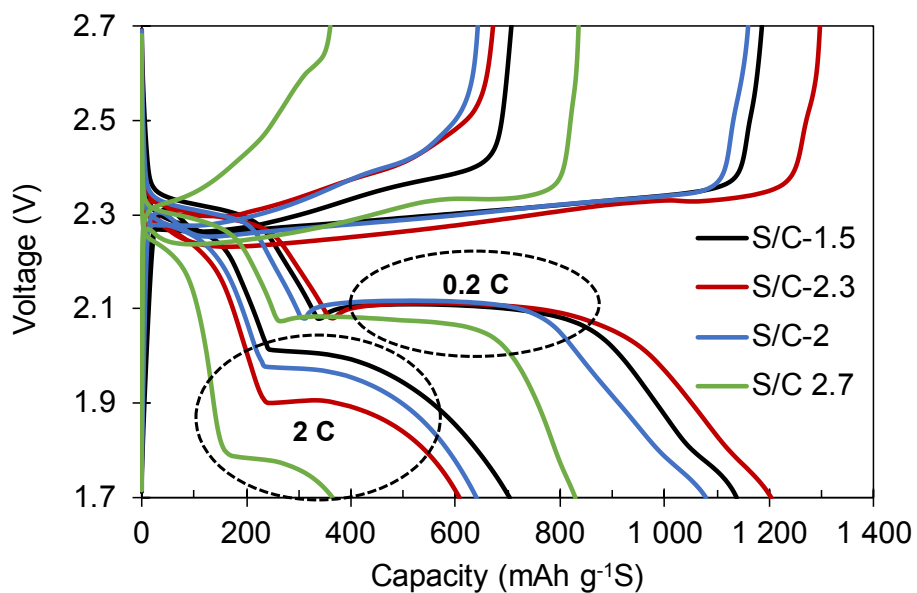


**Figure S8.** Comparison of the galvanostatic profiles of the S/C cathodes with different S contents showing higher polarization with the increase of S content and charge-discharge rate.

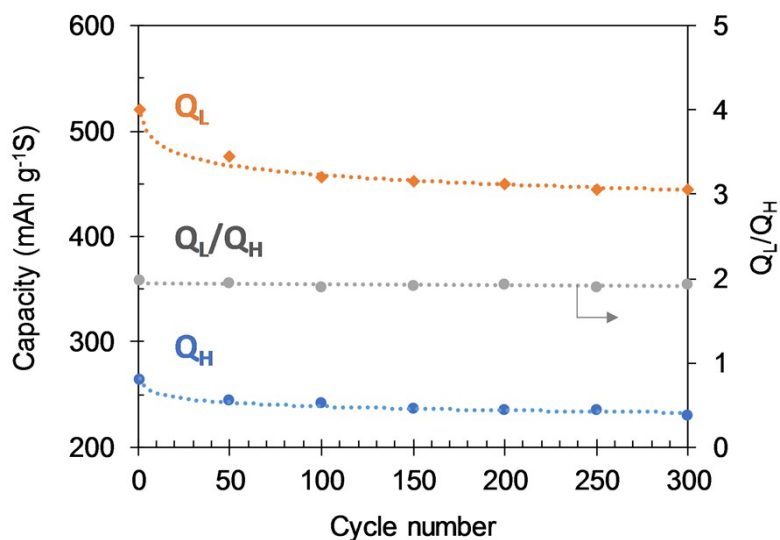


**Figure S9.** The evolution of the capacities corresponding to the upper plateau ( $Q_H$ ) and lower plateau ( $Q_L$ ) for the S/C-1.5 battery cycled at 1C, as well as the ratio between them ( $Q_L/Q_H$ ).

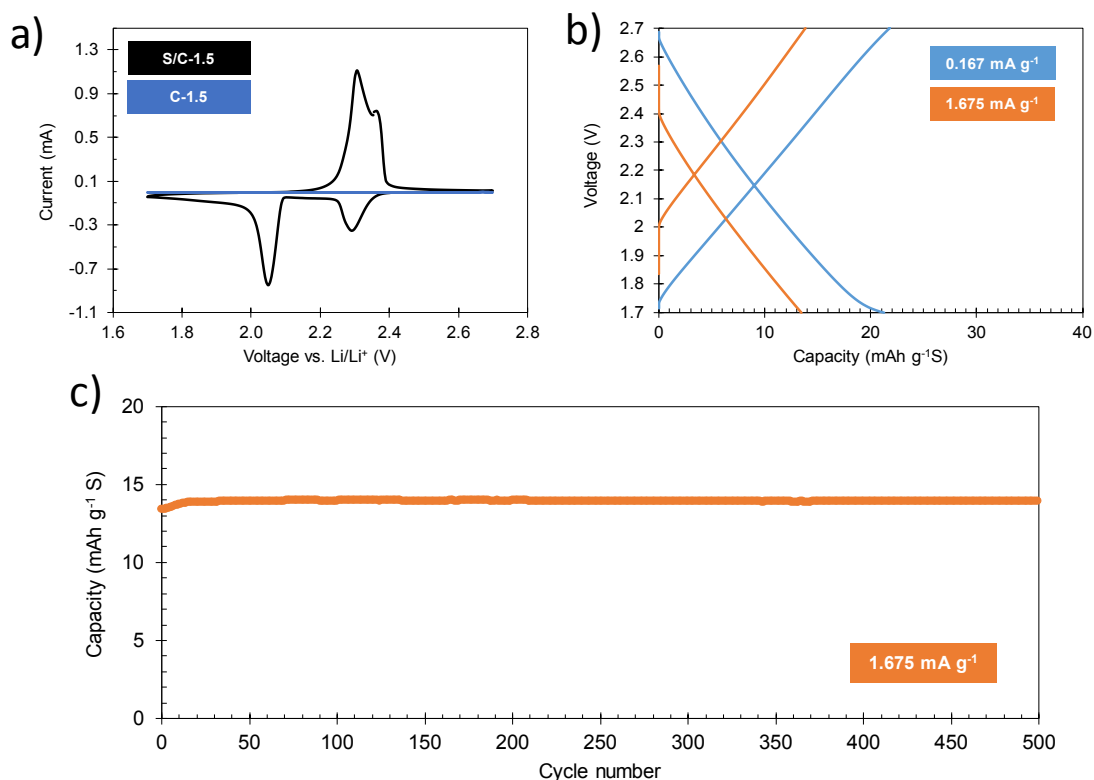


**Figure S10.** Electrochemical characterization of a battery using the C-1.5 carbon as the cathode material: (a) Cyclic voltammograms at  $0.05 \text{ mV s}^{-1}$  ( $10^{\text{th}}$  cycle; the plot corresponding to the S/C-1.5 composite is included as a reference); (b) galvanostatic charge-discharge profiles; (c) capacity retention during long charge-discharge cycling. Mass loading:  $1 \text{ mg cm}^{-2}$ .

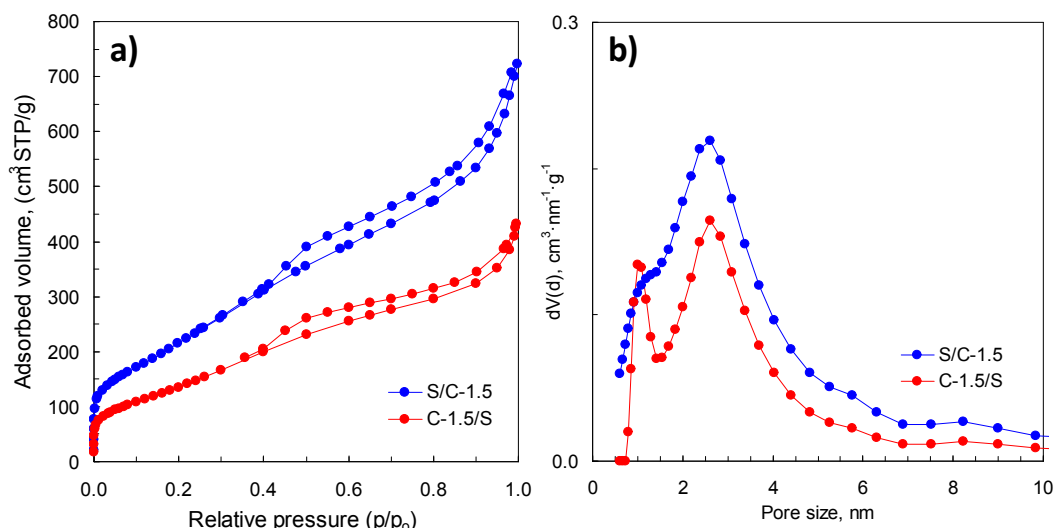


**Figure S11.** (a) Nitrogen sorption isotherms and (b) pore size distributions of the sulfur/carbon composites synthesized by the *in situ* procedure (S/C-15) and by means of melt infiltration (C-1.5/S). Sulfur amount: 52 %.

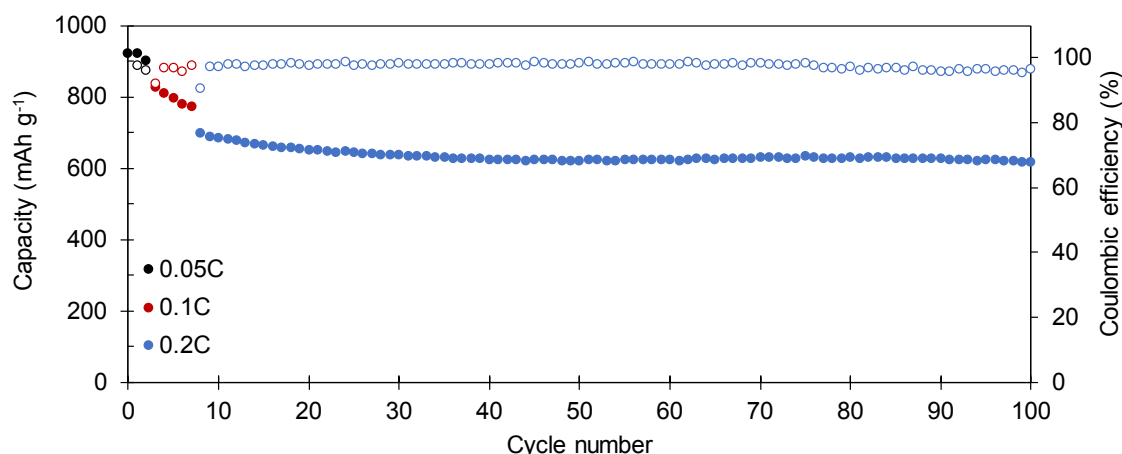


**Figure S12.** Cycling performance of S/C-2.3 (81.9 % S) at different charge-discharge rates. Areal sulfur loading: 7.1 mg cm<sup>-2</sup>.

**Table S1.** Physicochemical properties of sulfur-carbon composites obtained by *in situ* synthesis (S/C-1.5) and by melting infiltration (C-1.5/S). Amount of infiltrated sulfur: 52 %.

Sample code	$S_{\text{BET}}$ (m <sup>2</sup> g <sup>-1</sup> )	$V_p$ (cm <sup>3</sup> g <sup>-1</sup> ) <sup>a</sup>	$V_{\text{micro} < 2 \text{ nm}}$ (cm <sup>3</sup> g <sup>-1</sup> )	Electrical conductivity (S cm <sup>-1</sup> )
S/C-1.5	790	1.12 (1.02)	0.19	2.6
C-1.5/S	490	0.67 (1.02)	0.12	1.6

<sup>a</sup> The theoretical unoccupied pore volumes deduced by assuming that the sulfur is confined within the porosity of carbon are indicated in parentheses. This parameter was calculated by using the formula:  $[V_p \times (1 - a_s) - a_s / 2.07]$ ,  $a_s$  being the fraction of sulfur and 2.07 its density.

**Supplementary Note 1.** As detailed in the manuscript, in order to compare our *in situ* approach with the conventional melt-diffusion procedure, the composite C-1.5/S containing 52% of sulfur was also synthesized by the latter methodology. This composite was characterized by XRD and nitrogen physisorption. According to the XRD pattern of the C-1.5/S composite (not shown), the sulfur is entirely infiltrated within the pores during the melt-diffusion treatment (no peaks associated to elemental sulfur present). However, the nitrogen adsorption results presented in Figure S9 and Table S1 show that the sulfur-carbon composite fabricated according to the conventional melt-infiltration procedure exhibits poorer textural properties (lower specific BET surface area and pore volume) than the S/C samples synthesized by using our *in situ* methodology (S/C-1.5). Thus, the measured pore volume of  $0.67 \text{ cm}^3 \text{ g}^{-1}$  is considerably smaller than that of S/C-1.5 ( $1.12 \text{ cm}^3 \text{ g}^{-1}$ ) and the theoretical pore volume for a S/C composite with unobstructed pores (i.e.  $1.02 \text{ cm}^3 \text{ g}^{-1}$ ). These results indicate that the melt-infiltrated sulfur is found blocking the access to a significant number of pores, which strongly suggests that the sulfur is less homogeneously distributed within the pore network. The less intimate interaction between the infiltrated sulfur and the surface of the porous carbon seems to be the main reason for the worse retention of capacity upon cycling observed during the long-term galvanostatic charge-discharge tests (Figure 7e). This, together with the fact that the electrical conductivity of the C-1.5/S sample ( $1.6 \text{ S cm}^{-1}$ ) is notably lower than that of S/C-1.5 ( $2.6 \text{ S cm}^{-1}$ ), clearly suggests that the S/C-1.5 sample meets better the desirable features for its employ as a cathode in Li-S cells.